




 Cite this: *Chem. Commun.*, 2019, 55, 11735

 Received 29th July 2019,
 Accepted 30th August 2019

DOI: 10.1039/c9cc05884b

rsc.li/chemcomm

Inorganic–organic hybrid high-dimensional polyoxotantalates and their structural transformations triggered by water†

 Zhong Li, Jing Zhang, Li-Dan Lin, Jin-Hua Liu, Xin-Xiong Li * and Shou-Tian Zheng *

The first two inorganic–organic hybrid three-dimensional (3D) polyoxotantalates (POTas) and the first two inorganic–organic hybrid 2D POTas have been obtained. All of these high-dimensional POTas are built from a new-type POTa dimeric cluster $\{\text{Cu}(\text{en})(\text{Ta}_6\text{O}_{19})\}_2/\{\text{Cu}(\text{enMe})(\text{Ta}_6\text{O}_{19})\}_2$ (en = ethylenediamine, enMe = 1,2-diaminopropane) bridged by copper complexes. Interestingly, extended POTas **1** and **3** can undergo single-crystal to single-crystal structural transformations triggered by water.

Polyoxometalates (POMs) are a unique class of metal-oxide clusters derived from metal elements of V, Nb, Ta, Mo, and W, which have remarkable structural features and wide applications in catalysis, materials, biology, *etc.*¹ During the past two decades, the design and synthesis of POM-based high-dimensional (2D or 3D) organic–inorganic hybrid materials have been a research focus in POM chemistry.^{2–7} Up to now, chemists from all over the world have succeeded in synthesizing a large number of various fascinating high-dimensional materials built from polyoxovanadates (POVs),^{2,3} polyoxomolybdates (POMos),^{4,5} and polyoxotungstates (POTs).^{6,7} Some representative examples include 3D POMs $\{\{\text{Co}(\text{H}_2\text{O})_4\}_3\text{V}_{18}\text{O}_{42}(\text{XO}_4)\}_n$,^{2a} $\{\{\text{Cd}(\text{en})\}_4\text{Ge}_8\text{V}_{10}\text{O}_{46}(\text{H}_2\text{O})[\text{V}(\text{H}_2\text{O})_2]_4(\text{GeO}_2)_4\}_n$,^{3a} $[\text{Gd}(\text{H}_2\text{O})_3]_3[\text{GdMo}_{12}\text{O}_{42}]_n$,^{4a} (TBA)₃[PMo₁₂O₃₈(OH)₂Zn₄(IN)₂],^{5b} $\text{KH}_2[(\text{C}_5\text{H}_8\text{NO}_2)_4(\text{H}_2\text{O})\text{Cu}_3][\text{BW}_{12}\text{O}_{40}] \cdot 5\text{H}_2\text{O}$,^{6a} $\text{Li}_{18}\text{Mn}_8(\text{NH}_4)_6[\text{P}_8\text{W}_{48}\text{O}_{184}]_n$,^{7a} and so on.

Compared with the above well-known high-dimensional POVs, POMos and POTs, high-dimensional polyoxoniobates (PONBs) have been known just in recent years. Though starting relatively late, the study on the synthesis of extended PONBs has achieved rapid development. Many novel inorganic–organic hybrid high-dimensional frameworks based on various PONBs have been reported one after another,^{8,9} such as isopolyniobate-based 3D frameworks $(\text{H}_2\text{en})_6\{\{\text{Cu}(\text{en})_2(\text{H}_2\text{O})_2\}_3\{\{\text{Nb}_{24}\text{O}_{72}\text{H}_9\}\{\text{Cu}(\text{en})_2$

$(\text{H}_2\text{O})_2\}\text{Cu}(\text{en})_2\}_2\}_2\cdot 66\text{H}_2\text{O}^{8a}$ and $\text{Na}_4\text{K}_2\text{H}_{16}[\text{Cu}(\text{en})_2]_{0.5}\{\{\text{Cu}(\text{en})_2\}_{9.5}(\text{K} = \text{H}_3\text{Cu}_4(\text{en})\text{Nb}_{78}\text{O}_{222})\}_{23} \cdot 8\text{H}_2\text{O}^{8b}$ and some impressive heteropolyoxoniobate-based 3D frameworks $\{\{\text{Cu}_6\text{L}_6(\text{H}_2\text{O})_3\}[\text{Nb}_{10}\text{V}_4\text{O}_{40}(\text{OH})_2]_2\cdot 13\text{H}_2\text{O}^{9a}$, $[\text{Cu}(\text{en})_2]_4[\text{PNb}_{12}\text{O}_{40}(\text{VO})_6](\text{OH})_{58} \cdot \text{H}_2\text{O}^{9b}$ and $\{\text{V}^{\text{V}}(\text{H}_2\text{O})_6\}_{0.5}\{\text{Co}^{\text{II}}(\text{en})_2\}_4\{\text{SNb}_8\text{V}^{\text{IV}}_8\text{V}^{\text{V}}_{1.25}\text{O}_{45.25}\}(\text{OH})_{4.25} \cdot 3\text{H}_2\text{O}^{9c}$ *etc.* (L = 1,10-phenanthroline).

Polyoxotantalates (POTas), as an important branch of POMs, have promising applications in photocatalysis and conducting materials, and thus have gradually received the attention of material researchers.¹⁰ However, even after decades of research, the progress on the syntheses of new-type POTas is still very limited. In particular, most of the known POTas are discrete^{11–16} and low-dimensional^{12c} structures, such as $[\text{Ta}_6\text{O}_{19}\{\text{M}(\text{CO})_3\}_n]^{(8-n)-}$ (M = Mn, Re),¹¹ $[\text{Ta}_6\text{O}_{19}]^{8-}$,¹² $[\text{Ta}_{10}\text{O}_{28}]^{6-}$,¹³ $[\text{Ti}_2\text{Ta}_8\text{O}_{28}]^{8-}$,¹⁴ $[\text{Ti}_{12}\text{Ta}_4\text{O}_{44}]^{10-}$,¹⁴ $\{\text{Co}_8\text{Ta}_{24}\text{O}_{80}\}^{15}$ and $\{\text{Cp}^*\text{M}\}^{2+}$ (M = Rh, Ir, Ru) group modified $\{\text{Ta}_6\}$.¹⁶ So far, no high-dimensional POTas have been obtained. The main reason is the difficulty in synthesis due to the low solubility and inert nature of tantalate species.¹⁷ Therefore, the exploration of new-type POTas for the construction of extended structures remains a great challenge.

Herein, we report a series of novel inorganic–organic hybrid high-dimensional POTa materials, including $\text{H}_2[\text{Cu}(\text{en})_2(\text{H}_2\text{O})_2]\cdot\{\{\text{Cu}(\text{en})_2\}_4[\text{Cu}(\text{en})(\text{Ta}_6\text{O}_{19})_2]\}_2\cdot 14\text{H}_2\text{O}$ (**1**), $\text{H}_2\{\{\text{Cu}(\text{en})_2\}_3[\text{Cu}(\text{en})(\text{H}_2\text{O})_2\text{Cu}(\text{en})(\text{Ta}_6\text{O}_{19})_2]\}_2\cdot 30\text{H}_2\text{O}$ (**2**), $\text{H}_2[\text{Cu}(\text{enMe})_2(\text{H}_2\text{O})_2][\text{Na}_2(\text{H}_2\text{O})_{10}]_2\{\{\text{Cu}(\text{enMe})_2\}_2[\text{Cu}(\text{enMe})(\text{Ta}_6\text{O}_{19})_2]\}_2\cdot 26\text{H}_2\text{O}$ (**3**), and $\text{H}_4[\text{Na}_4(\text{H}_2\text{O})_{18}]\{\{\text{Cu}(\text{enMe})_2\}_2[\text{Cu}(\text{enMe})(\text{Ta}_6\text{O}_{19})_2]\}_2\cdot 10\text{H}_2\text{O}$ (**4**) (en = ethylenediamine, enMe = 1,2-diaminopropane). As far as we know, **1** and **2** are the first two 3D POTas, while **3** and **4** are the first two 2D POTas. All these compounds are based on unique inorganic–organic hybrid dimeric POTa cluster secondary building units (SBUs) $[\text{Cu}(\text{en})(\text{Ta}_6\text{O}_{19})_2]^{12-}/[\text{Cu}(\text{enMe})(\text{Ta}_6\text{O}_{19})_2]^{12-}$ (denoted as $\{\text{CuTa}_6\}_2$). Interestingly, **1** and **3** can undergo single-crystal (SC) to single-crystal structural transformations triggered by water.

Single-crystal X-ray diffraction (SCXRD) analysis reveals that **1** crystallizes in the monoclinic space group $P2_1/c$, and its asymmetric unit consists of half of a $\{\text{CuTa}_6\}_2$ SBU, two $[\text{Cu}(\text{en})_2]^{2+}$ complexes and half of a $[\text{Cu}(\text{en})_2(\text{H}_2\text{O})]^{2+}$ cation.

State Key Laboratory of Photocatalysis on Energy and Environment,
 College of Chemistry, Fuzhou University, Fuzhou 350108, Fujian, China.
 E-mail: lxx@fzu.edu.cn, stzheng@fzu.edu.cn

† Electronic supplementary information (ESI) available. CCDC 1866075–1866080. For ESI and crystallographic data in CIF or other electronic format see DOI: 10.1039/c9cc05884b

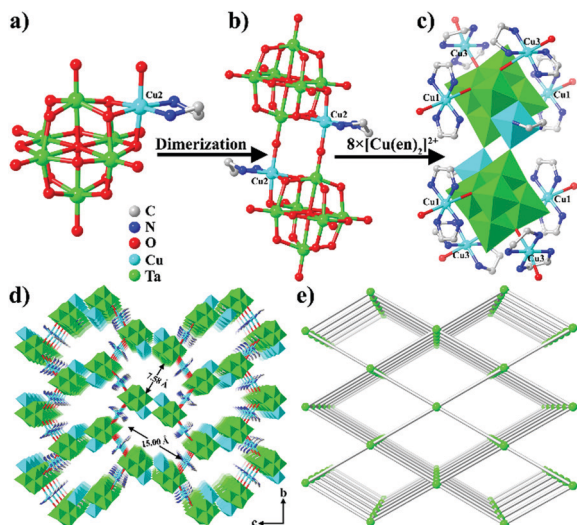


Fig. 1 (a) The $[\text{Cu}(\text{en})(\text{Ta}_6\text{O}_{19})]^{6-}$ cluster; (b) the structure of the $\{\text{CuTa}_6\}_2$ SBU; (c) the coordination environment of the $\{\text{CuTa}_6\}_2$ SBU; (d) view of the 3D framework structure in **1**; (e) the 3D framework topology of **1**. Polyhedral codes: TaO_6 , green; $\text{CuO}_2\text{N}_4/\text{CuO}_4\text{N}_2$, cyan.

$\{\text{CuTa}_6\}_2$ is composed of two centrosymmetric mono-copper capped Lindqvist-type POTa clusters (Fig. 1a), in which the octahedral copper ion is captured by one $\{\text{Ta}_3\text{O}_3\}$ group of a $\{\text{Ta}_6\text{O}_{19}\}$ cluster through three bridging oxygen atoms. The rest of the coordination sites of the copper ion are finished by two N donors from one chelating en ligand and one terminal oxo atom from a neighboring $\{\text{Ta}_6\text{O}_{19}\}$ cluster (Fig. 1b). It is noteworthy that such a dimeric structure is very rare among reported POTas,^{11–16} although a discrete dimeric POTa $\{[(\text{C}_6\text{H}_6)\text{RuTa}_6\text{O}_{18}]_2(\mu\text{-O})\}^{10-}$ has been reported in 2014.^{16a} The $\{\text{CuTa}_6\}_2$ cluster not only enriches the cluster diversity of the POTa family, but also provides a potential SBU for making high-dimensional POTas. In **1**, each $\{\text{CuTa}_6\}_2$ cluster is surrounded by eight $[\text{Cu}(\text{en})_2]^{2+}$ complexes (four Cu1 and four Cu3 complexes) to join with six neighboring $\{\text{CuTa}_6\}_2$ clusters (Fig. 1c). The bond distances of Cu–O, Cu–N and Ta–O bonds are in the range of 1.948–2.876 Å, 2.043–2.083 Å and 1.780–2.409 Å, respectively. The axial Cu–O bonds are much longer than the equatorial Cu–N bonds, which is ascribed to the presence of the Jahn–Teller effect.¹⁸ The $\{\text{CuTa}_6\}_2$ SBUs are first bridged by Cu3 complexes to form a 2D layer (Fig. S1, ESI[†]), and the neighboring symmetry-related layers are further integrated by Cu1 complexes (Fig. S2, ESI[†]), resulting in the formation of a 3D anionic framework (Fig. 1d). The framework possesses large irregular 1D channels along the *a* axis, which are filled with dissociative $[\text{Cu}(\text{en})_2(\text{H}_2\text{O})_2]^{2+}$ cations and lattice water molecules (Fig. S3, ESI[†]). From the topological point of view, the $\{\text{CuTa}_6\}_2$ SBUs can be regarded as six-connected nodes, and the whole framework can be simplified as a *pcu*-type topology (Fig. 1e).

The successful construction of **1** indicates that $\{\text{CuTa}_6\}_2$ is a suitable SBU for making high-dimensional POTa-based framework materials. Interestingly, when the crystals of **1** were immersed in water and left for slow evaporation for a few days,

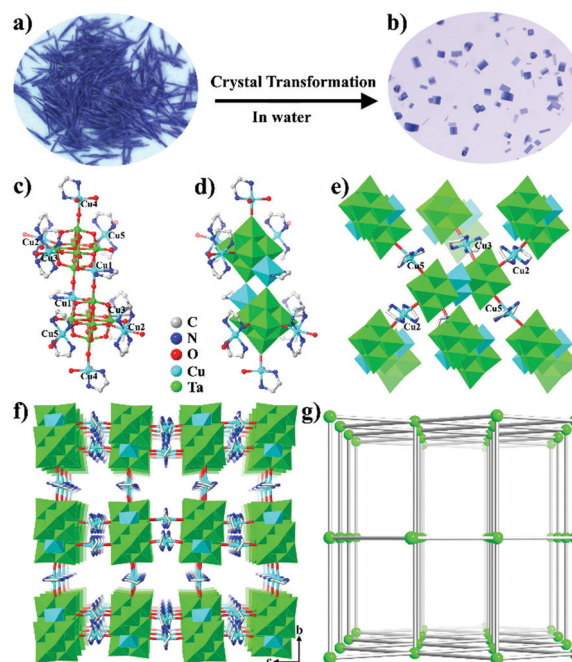


Fig. 2 (a and b) Crystals **1** (left) and **2** (right); (c and d) coordination environment of the $\{\text{CuTa}_6\}_2$ SBU in **2**; (e) the linking mode of the $\{\text{CuTa}_6\}_2$ SBU in **2**; (f and g) view of the 3D framework and its topology in **2**. Polyhedral codes: TaO_6 , green; CuO_2N_4 , cyan.

the $\{\text{CuTa}_6\}_2$ SBUs undergo a recombination process, and the framework of **1** can transform into a different framework of **2**. As shown in Fig. 2a and b, as the framework transformed, the bar-shaped crystals of **1** simultaneously transform into block-shaped crystals of **2**. SCXRD analysis indicates that the linkages of $\{\text{CuTa}_6\}_2$ SBUs and $[\text{Cu}(\text{en})_2]^{2+}$ bridges in the new 3D framework are different from that in **1**. There are also eight copper complexes on the exterior of each $\{\text{CuTa}_6\}_2$ SBU, including two decorative five-coordinated $[\text{Cu}(\text{en})(\text{H}_2\text{O})_2]^{2+}$ cations and six bridging $[\text{Cu}(\text{en})_2]^{2+}$ complexes (Fig. 2c and d). But, each $\{\text{CuTa}_6\}_2$ SBU connects to the neighboring six ones only through six $[\text{Cu}(\text{en})_2]^{2+}$ complexes to generate a 3D anionic framework with *pcu*-type topology (Fig. 2e–g). Although the frameworks of **1** and **2** share the same topology, there are still several obvious discrepancies between them. First, the number of $[\text{Cu}(\text{en})_2]^{2+}$ bridges used to connect each $\{\text{CuTa}_6\}_2$ SBU in **1** is eight, while the number of that in **2** is only six. Secondly, the framework of **1** is charge balanced by isolated $[\text{Cu}(\text{en})_2(\text{H}_2\text{O})_2]^{2+}$ complexes located in 1D channels, while that of **2** is balanced by decorative $[\text{Cu}(\text{en})(\text{H}_2\text{O})_2]^{2+}$ complexes derived from the $\{\text{CuTa}_6\}_2$ SBU, besides the delocalized protons in both compounds. Thirdly, the shapes of the 1D channels in the two frameworks are obviously different. The existence of these differences further testifies that the dimeric $\{\text{CuTa}_6\}_2$ cluster is a flexible SBU in assembling extended framework materials.

Besides 3D frameworks, the dimeric $\{\text{CuTa}_6\}_2$ cluster can also be employed as a SBU to construct 2D layered materials. By maintaining the reaction conditions similar with those used for **1**, and by replacing en with enMe, lamellar purple crystals of **3** were obtained (Fig. S4, ESI[†]). The SCXRD study indicates that each $\{\text{CuTa}_6\}_2$ SBU is surrounded by four $[\text{Cu}(\text{enMe})_2]^{2+}$

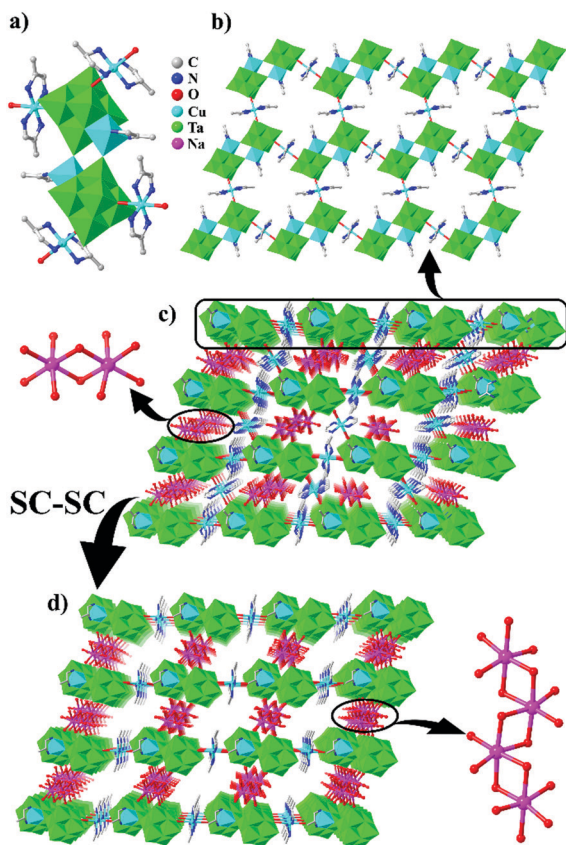


Fig. 3 (a) Coordination environment of the $\{\text{CuTa}_6\}_2$ SBU in **3**; (b) the structure of the 2D layer in **3**; (c) the stacking style of 2D layers in **3**, and the charge balancing cations between two neighboring layers; (d) the stacking style of 2D layers in **4**, and the charge balancing cations between two neighboring layers. Polyhedral codes: TaO_6 , green; $\text{CuO}_2\text{N}_4/\text{CuO}_4\text{N}_2$, cyan.

complexes to form a 2D anionic layer structure (Fig. 3a and b). The layers stack in parallel with an interlayer distance of about 5.800 Å, and the interspaces are filled with charge balancing cations including novel $[\text{Na}_2(\text{H}_2\text{O})_{10}]^{2+}$ clusters and $[\text{Cu}(\text{enMe})_2(\text{H}_2\text{O})_2]^{2+}$ complexes (Fig. 3c). The 2D layers cannot be further joined by $[\text{Cu}(\text{enMe})_2(\text{H}_2\text{O})_2]^{2+}$ complexes to form a 3D framework structure maybe ascribed to the steric hindrance of the methyl group on enMe. Intriguingly, when crystals of **3** are soaked in water, they can partially transform into crystals of **4** (Fig. S4, ESI[†]). The SCXRD study reveals that **4** contains the same 2D anionic layer as that in **3**. The most noticeable difference between **3** and **4** is that the charge compensation cation $[\text{Na}_2(\text{H}_2\text{O})_{10}]^{2+}$ clusters and $[\text{Cu}(\text{enMe})_2(\text{H}_2\text{O})_2]^{2+}$ complexes in **3** are replaced by $[\text{Na}_4(\text{H}_2\text{O})_{18}]^{4+}$ clusters in **4** (Fig. 3d). To our knowledge, the studies of SC to SC transformations have remained unexplored in POTa chemistry. The structural transformation studies of **1** to **2** and **3** to **4** will inevitably provide useful kinetic references in understanding dynamic properties of tantalate clusters.

The successful construction of **1–4** shows that the $\{\text{CuTa}_6\}_2$ cluster is a good SBU in making high-dimensional POTa materials. As a matter of fact, the $\{\text{CuTa}_6\}_2$ cluster is also suitable to construct low-dimensional POTa materials. During our exploration, we

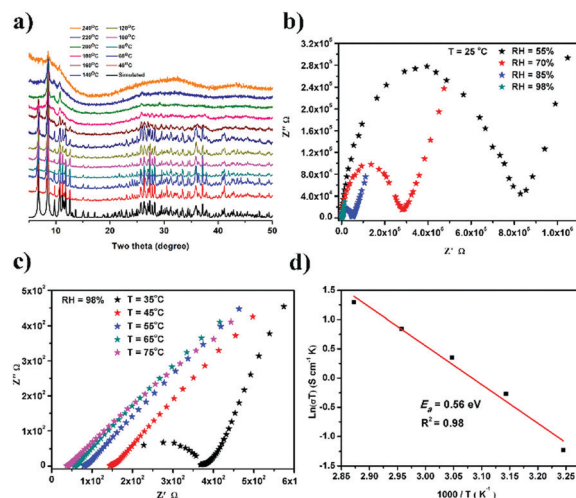


Fig. 4 (a) Variable-temperature PXRD patterns of the as-synthesized sample **1**; (b) Nyquist plots for **1** under different RH conditions at 25 °C; (c) Nyquist plots for **1** under different temperature conditions at 98% RH; (d) Arrhenius plots and linear fitting of temperature-dependence proton conduction at 98% RH.

also obtained another two 1D POTas with the formula of $\text{H}_2[\text{Cu}(\text{en})_2(\text{H}_2\text{O})_2]\{[\text{Cu}(\text{en})_2]_2[\text{Na}_2(\text{H}_2\text{O})_7]_2[\text{Cu}(\text{en})(\text{Ta}_6\text{O}_{19})]_2\} \cdot 10\text{H}_2\text{O}$ (**5**) and $\text{H}_2[\text{Na}_2(\text{H}_2\text{O})_{10}]_2[\text{Cu}(\text{en})_2]_2\{[\text{Cu}(\text{en})]_2[\text{Cu}(\text{en})(\text{Ta}_6\text{O}_{19})]_2\} \cdot 8\text{H}_2\text{O}$ (**6**) (Fig. S5, ESI[†]). The dimensional diversity of compounds **1–6** confirms the great potential for creating a large family of new POTas by using $\{\text{CuTa}_6\}_2$ as a SBU. The solvothermally prepared crystals of **1** and **3** were selected as examples for investigating thermal stabilities of our materials. As shown in Fig. 4a, variable-temperature powder X-ray diffraction (PXRD) patterns show that the framework of **1** retains its crystallinity up to 160 °C. However, the crystallinity of **3** was lost when the temperature rises to 80 °C (Fig. S7, ESI[†]).

The high yield, high stability and the incorporation of massive lattice water molecules within the 1D channels of the framework prompted us to study the proton-conducting ability of **1**. The proton conductivity of **1** was measured *via* alternating current impedance spectroscopy by using a two electrode configuration in the temperature range spanning from 25 °C to 75 °C and under relative humidity (RH) ranging from 55% RH to 98% RH. The bulk conductivities were calculated using the equation ($\sigma = L/RS$), where σ , R , L and S are bulk conductivity (S cm^{-1}), fitting resistance (Ω), thickness (cm) and cross-sectional area (cm^2) of the sandwiched sample, respectively. As shown in Fig. 4b, when RH gradually enhances from 55% to 98% at 25 °C, the conductivity increases from $4.29 \times 10^{-7} \text{ S cm}^{-1}$ to $9.90 \times 10^{-5} \text{ S cm}^{-1}$, which indicates that the enhancement of humidity does not have a significant impact on accelerating the proton-conducting rates. Furthermore, the temperature-dependent behaviors are measured at 98% RH. As shown in Fig. 4c, when the temperature increases from 35 °C to 75 °C, the conductivity increases remarkably and reaches the maximum value of $1.04 \times 10^{-2} \text{ S cm}^{-1}$ at 75 °C. Such a behavior can be ascribed to the fact that the velocity of water molecules in the channels is accelerated as the temperature increases. The activation

energy (E_a) was evaluated using the Arrhenius equation $\sigma T = \sigma_0 \exp(E_a/k_b T)$. Determined by linear regression analysis, the E_a of **1** was calculated to be 0.56 eV (Fig. 4d), known as a Vehicular mechanism (>0.4 eV).¹⁹ Compared with reported POM-based proton-conducting materials (Table S2, ESI[†]), the performance of **1** is superior to most reported compounds.²⁰

To summarise, the first series of high-dimensional extended inorganic–organic hybrid POTas have been created under solvothermal conditions. All compounds are constructed from novel dimeric $\{\text{CuTa}_6\}_2$ cluster SBUs and different numbers of $[\text{Cu}(\text{en})_2]^{2+}/[\text{Cu}(\text{enMe})_2]^{2+}$ bridges. Interestingly, compounds **1** and **3** show uncommon SC to SC structural transformations triggered by water. The successful syntheses of these new POTas not only enrich the rather limited structural diversity of POTas, but also provide useful references for further developing POTa chemistry. Considering the flexible linking characteristic of $\{\text{CuTa}_6\}_2$ cluster SBUs, we believe that a large family of new POTa-based extended materials will be made in the near future.

We gratefully acknowledge the financial support from the Natural Science Foundation of China (No. 21671040, 21971039 and 21773029).

Conflicts of interest

There are no conflicts to declare.

Notes and references

- (a) D. Y. Du, L. K. Yan, Z. M. Su, S. L. Li, Y. Q. Lan and E. B. Wang, *Coord. Chem. Rev.*, 2013, **257**, 702; (b) X. X. Li, Y. X. Wang, R. H. Wang, C. Y. Cui, C. B. Tian and G. Y. Yang, *Angew. Chem., Int. Ed.*, 2016, **55**, 6462; (c) S. S. Wang and G. Y. Yang, *Chem. Rev.*, 2015, **115**, 4893; (d) H. N. Miras, L. Vila Nadal and L. Cronin, *Chem. Soc. Rev.*, 2014, **43**, 5679; (e) Z. Li, L. D. Lin, H. Yu, X. X. Li and S. T. Zheng, *Angew. Chem., Int. Ed.*, 2018, **57**, 15777; (f) A. Bijelic, M. Aureliano and A. Rompel, *Chem. Commun.*, 2018, **54**, 1153; (g) X. X. Li, D. Zhao and S. T. Zheng, *Coord. Chem. Rev.*, 2019, **397**, 220.
- (a) M. I. Khan, E. Yohannes and R. J. Doedens, *Angew. Chem., Int. Ed.*, 1999, **38**, 1292; (b) C. L. Chen, A. M. Goforth, M. D. Smith, C. Y. Su and H. C. zur Loye, *Angew. Chem., Int. Ed.*, 2005, **44**, 6673; (c) Y. Q. Lan, S. L. Li, Z. M. Su, K. Z. Shao, J. F. Ma, X. L. Wang and E. B. Wang, *Chem. Commun.*, 2008, 58.
- (a) J. Zhou, J. W. Zhao, Q. Wei, J. Zhang and G. Y. Yang, *J. Am. Chem. Soc.*, 2014, **136**, 5065; (b) X. X. Li, L. J. Zhang, C. Y. Cui, R. H. Wang and G. Y. Yang, *Inorg. Chem.*, 2018, **57**, 10323; (c) H. Chen, Z. B. Yu, Z. Bacsik, H. S. Zhao, Q. X. Yao and J. L. Sun, *Angew. Chem., Int. Ed.*, 2014, **53**, 3608.
- (a) C. D. Wu, C. Z. Lu, H. H. Zhuang and J. S. Huang, *J. Am. Chem. Soc.*, 2002, **124**, 3836; (b) J. Chen, S. F. Lu, R. M. Yu, Z. N. Chen, Z. X. Huang and C. Z. Lu, *Chem. Commun.*, 2002, 2640; (c) E. Burkholder, V. Golub, C. J. O'Connor and J. Zubieta, *Chem. Commun.*, 2003, 2128; (d) H. Q. Tan, G. Y. Li, Z. M. Zhang, C. Qin, X. L. Wang, B. E. Wang and M. Z. Su, *J. Am. Chem. Soc.*, 2007, **129**, 10066.
- (a) A. Macdonell, N. A. B. Johnson, A. J. Surman and L. Cronin, *J. Am. Chem. Soc.*, 2015, **137**, 5662; (b) Y. Y. Wang, M. Zhang, S. L. Li, S. R. Zhang, W. Xie, J. S. Qin, Z. M. Su and Y. Q. Lan, *Chem. Commun.*, 2017, **53**, 5204; (c) X. X. Li, F. C. Shen, J. Liu, S. L. Li, L. Z. Dong, Q. Fu, Z. M. Su and Y. Q. Lan, *Chem. Commun.*, 2017, **53**, 10054.
- (a) H. Y. An, E. B. Wang, D. R. Xiao, Y. G. Li, Z. M. Su and L. Xu, *Angew. Chem., Int. Ed.*, 2006, **45**, 904; (b) C. Streb, C. Ritchie, D. L. Long, P. Kogerler and L. Cronin, *Angew. Chem., Int. Ed.*, 2007, **46**, 7579; (c) C. Ritchie, E. M. Burkholder, D. L. Long, D. Adam, P. Kogerler and L. Cronin, *Chem. Commun.*, 2007, 468.
- (a) T. Boyd, S. G. Mitchell, D. Gabb, D. L. Long, Y. F. Song and L. Cronin, *J. Am. Chem. Soc.*, 2017, **139**, 5930; (b) C. C. Zhao, E. N. Glass, B. Chica, D. G. Musaev, J. M. Sumliner, R. B. Dyer, T. Q. Lian and C. L. Hill, *J. Am. Chem. Soc.*, 2014, **136**, 12085; (c) E. D. Koutsouroubi, A. K. Xylouri and G. S. Armatas, *Chem. Commun.*, 2015, **51**, 4481.
- (a) R. P. Bontchev and M. Nyman, *Angew. Chem., Int. Ed.*, 2006, **45**, 6670; (b) L. Jin, Z. K. Zhu, Y. L. Wu, Y. J. Qi, X. X. Li and S. T. Zheng, *Angew. Chem., Int. Ed.*, 2017, **56**, 16288; (c) J. Y. Niu, P. T. Ma, H. Y. Niu, J. Li, J. W. Zhao, Y. Song and J. P. Wang, *Chem. – Eur. J.*, 2007, **13**, 8739.
- (a) P. Huang, C. Qin, X. L. Wang, C. Y. Sun, G. S. Yang, K. Z. Shao, Y. Q. Jiao, K. Zhou and Z. M. Su, *Chem. Commun.*, 2012, **48**, 103; (b) J. Q. Shen, Y. Zhang, Z. M. Zhang, Y. G. Li, Y. Q. Gao and E. B. Wang, *Chem. Commun.*, 2014, **50**, 6017; (c) J. F. Hu, T. Han, Y. N. Chi, Z. G. Lin, Y. Q. Xu, S. Yang, D. Wei, Y. Z. Zheng and C. W. Hu, *Chem. Commun.*, 2016, **52**, 10846.
- (a) J. L. Krinsky, L. L. Anderson, J. Arnold and R. G. Bergman, *Angew. Chem., Int. Ed.*, 2007, **46**, 369; (b) S. J. Li, S. M. Liu, S. X. Liu, Y. W. Liu, Q. Tang, Z. Shi, S. X. Ouyang and J. H. Ye, *J. Am. Chem. Soc.*, 2012, **134**, 19716; (c) P. Huang, C. Qin, Y. Zhou, Y. M. Hong, X. L. Wang and Z. M. Su, *Chem. Commun.*, 2016, **52**, 13787.
- A. V. Besserguenev, M. H. Dickman and M. T. Pope, *Inorg. Chem.*, 2001, **40**, 2582.
- (a) L. Shen, Y. Q. Xu, Y. Z. Gao, F. Y. Cui and C. W. Hu, *J. Mol. Struct.*, 2009, **934**, 37; (b) P. A. Abramov, A. M. Abramova, E. V. Peresypkina, A. L. Gushchin, S. A. Adonin and M. N. Sokolov, *J. Struct. Chem.*, 2011, **52**, 1012; (c) G. L. Guo, Y. Q. Xu, B. K. Chen, Z. G. Lin and C. W. Hu, *Inorg. Chem. Commun.*, 2011, **14**, 1448; (d) S. N. Britvin, O. I. Sidra, A. Lotnyk, L. Kienle, S. V. Krivovichev and W. Depmeier, *Inorg. Chem. Commun.*, 2012, **25**, 18; (e) M. Matsumoto, Y. Ozawa and A. Yagasaki, *Inorg. Chem.*, 2012, **51**, 5991.
- M. Matsumoto, Y. Ozawa, A. Yagasaki and Y. Zhe, *Inorg. Chem.*, 2013, **52**, 7825.
- J. H. Son and W. H. Casey, *Chem. – Eur. J.*, 2016, **22**, 14155.
- Z. J. Liang, S. F. Zhao, P. T. Ma, C. Zhang, J. J. Sun, T. T. Song, J. Y. Niu and J. P. Wang, *Inorg. Chem.*, 2018, **57**, 12471.
- (a) P. A. Abramov, M. N. Sokolov, S. Floquet, M. Haouas, F. Taulelle, E. Cadot, E. V. Peresypkina, A. V. Virovets, C. Vicent, N. B. Kompankov, A. A. Zhdanov, O. V. Shuvaeva and V. P. Fedin, *Inorg. Chem.*, 2014, **53**, 12791; (b) P. A. Abramov, M. N. Sokolov, A. V. Virovets, S. Floquet, M. Haouas, F. Taulelle, E. Cadot, C. Vicent and V. P. Fedin, *Dalton Trans.*, 2015, **44**, 2234; (c) P. A. Abramov, C. Vicent, N. B. Kompankov, A. L. Gushchin and M. N. Sokolov, *Eur. J. Inorg. Chem.*, 2016, 154.
- (a) T. M. Anderson, M. A. Rodriguez, F. Bonhomme, J. N. Bixler, T. M. Alama and M. Nyman, *Dalton Trans.*, 2007, 4517; (b) M. Nyman and P. C. Burns, *Chem. Soc. Rev.*, 2012, **41**, 7354; (c) L. B. Fullmer, P. I. Molina, M. R. Antonio and M. Nyman, *Dalton Trans.*, 2014, **43**, 15295.
- (a) Z. Li, X. X. Li, T. Yang, Z. W. Cai and S. T. Zheng, *Angew. Chem., Int. Ed.*, 2017, **56**, 2664; (b) J. Y. Niu, X. A. Fu, J. W. Zhao, S. Z. Li, P. T. Ma and J. P. Wang, *Cryst. Growth Des.*, 2010, **10**, 3110.
- (a) K. D. Kreuer, *Chem. Mater.*, 1996, **8**, 610; (b) S. Chand, S. M. Elahi, A. Pal and M. C. Das, *Chem. – Eur. J.*, 2019, **25**, 6259.
- (a) J. C. Liu, Q. Han, L. J. Chen, J. W. Zhao, C. Streb and Y. F. Song, *Angew. Chem., Int. Ed.*, 2018, **57**, 8416; (b) P. T. Ma, R. Wan, Y. Y. Wang, F. Hu, D. D. Zhang, J. Y. Niu and J. P. Wang, *Inorg. Chem.*, 2016, **55**, 918; (c) Q. Gao, X. L. Wang, J. Xu and X. H. Bu, *Chem. – Eur. J.*, 2016, **22**, 9082.